Crystalline and Solution Phases in *N*,*N*,*N*′,*N*′,*N*′′-Pentamethyldiethylenetriamine with $LiCF_3SO_3$ and $NaCF_3SO_3$

Rebecca A. Sanders, Roger Frech,* and Masood A. Khan

Department of Chemistry and Biochemistry, University of Oklahoma, Norman, Oklahoma 73019

Received: December 31, 2003

Linear poly(*N*-methylethylenimine), LPMEI, a methylated derivative of linear poly(ethylenimine), shows potential as a polymer electrolyte host. The interactions of LPMEI with lithium and sodium cations are modeled by solutions of *N*,*N*,*N*′,*N*′,*N*′′-pentamethyldiethylenetriamine, PMDETA, containing either dissolved $LiCF_3SO_3$ (LiTf) or $NaCF_3SO_3$ (NaTf). During these studies, crystalline compounds were discovered and characterized by differential scanning calorimetry, Fourier transform infrared spectroscopy (IR), and Raman spectroscopy. Crystals of the NaTf complex, (PMDETA)NaTf, were of sufficient size to allow a structure determination by X-ray diffraction. The (PMDETA)NaTf crystallizes as two dimers with different symmetries in a monoclinic unit cell in the $P2_1/c$ space group. A spectroscopic comparison of PMDETA, the crystalline complex PMDETA−LiTf, crystalline (PMDETA)NaTf, and their corresponding salt solutions over a composition range of 1.7:1 to 6.7:1 (PMDETA:MTf molar ratio, $M = Li^+$, Na^+) was carried out with IR and Raman spectroscopy. The dominant species in the $(PMDETA)_x$NaTf solutions is the triple cation $[Na_2Tf]^+$, even at a 6.7:1 PMDETA:NaTf molar composition.

1. Introduction

The most widely studied polymer electrolyte is poly(ethylene oxide), PEO, complexed with various salts, such as $LiCF_3SO_3$, $LiN(CF_3SO_2)_2$, $LiSbF_6$, $LiBF_4$, and $LiClO_4$. The mechanism of ionic transport in these systems is not well-understood at the molecular level, although cation−anion interactions[1] and cation−polymer interactions[2] play a major role. Cation−polymer interactions lead to changes of the polymer backbone conformation,[3] while cation−anion interactions result in the formation of associated ionic species.[1,4] Thus, local structures (ionically associated species and local backbone conformation) may be used to study these important interactions and provide essential insight needed to understand the mechanism of ionic transport. Model compounds have proven useful in fundamental studies of local structures in polymer electrolytes. Model compounds for PEO-based electrolytes include the dimethyl ethers of ethylene oxides ($CH_3(OCH_2CH_2)_nOCH_3$, $n = 1-4$), otherwise known as glymes, i.e., monoglyme, diglyme, triglyme, and tetraglyme[3,5−10]

Linear poly(ethylenimine), LPEI, is a highly crystalline polymer that is structurally analogous to PEO. LPEI-based electrolytes exhibit poor conductivity because of the crystallinity of the host matrix. Despite this drawback, there have been attempts to understand ionic association and ion−polymer interactions in LPEI complexed with lithium and sodium salts. These attempts have been aided by the use of salt complexes of *N*,*N*′-dimethylethylenediamine.[11−14]

The addition of side chains (e.g., $-CH_3$, $-CH_2CH_3$) to LPEI decreases the crystallinity. Linear poly(*N*-methylethylenimine), LPMEI, is a methyl-substituted derivative of LPEI and is completely amorphous at room temperature, unlike LPEI, which melts at 58 °C.[15−17] Tanaka et al. studied the ionic conductivities of PMEI−$LiCF_3SO_3$ and PMEI−$LiClO_4$ electrolytes as a function of temperature and salt composition, comparing their behavior with that of the corresponding PEI-based electrolytes.[18] The authors concluded that the conductivities depended primarily on the Tg values at higher salt concentrations and pointed out that the conductivity values were "comparable with mediocre values for PEO−Li salt systems". In a later study, Sanders et al. also reported conductivity values for PMEI−$LiCF_3SO_3$ at two temperature and several salt compositions,[19] although the focus of the study was on the vibrational spectroscopy of the electrolyte system. That work was handicapped by the lack of reliable vibrational assignments in the PMEI-salt and the local structures responsible for certain modes. The LPMEI-based electrolytes have been explored by Tanaka et al.[17,18,20] and Sanders et al.[21]

There is very limited knowledge about the local structures in LPMEI; therefore, model compounds that mimic local structures and their associated vibrational modes in LPMEI and LPMEI-based polymer electrolytes would be useful. *N*,*N*,*N*′,*N*′-Tetramethylethylenediamine (TMEDA), which can be viewed as monomeric LPMEI, has been investigated by Sanders et al. as a possible model compound for LPMEI.[22] However, the short chain length of TMEDA limits its usefulness. Therefore, *N*,*N*,*N*′,*N*′,*N*′′-pentamethyldiethylenetriamine (PMDETA), which is essentially LPMEI with two repeat units, was investigated.[23,24] While studying solutions of PMDETA with $LiCF_3SO_3$ (LiTf) and $NaCF_3SO_3$ (NaTf), crystalline compounds were discovered. This paper characterizes the crystalline and amorphous phases in PMDETA−LiTf and PMDETA−NaTf systems, using X-ray diffraction, Fourier transform infrared spectroscopy (IR), Raman spectroscopy, and differential scanning calorimetry (DSC). Structural information obtained from the (PMDETA)NaTf crystal provides a better understanding of the local environment of PMDETA and the triflate anion in the $(PMDETA)_x$NaTf solutions (x = various molar compositions).

2. Experimental Section

2.1. Sample Preparation. *N*,*N*,*N*′,*N*′,*N*′′-Pentamethyldiethylenetriamine (PMDETA), LiTf, and NaTf were obtained from

* Corresponding author. Phone: 1-405-325-3831. Fax: 1-405-325-6111. E-mail: rfrech@ou.edu.

10.1021/jp0313526 CCC: $27.50
Published on Web 07/31/2004

Aldrich. PMDETA was distilled over sodium metal. LiTf and NaTf were heated under vacuum at 120 °C for 48 h. The chemicals were stored and used in a dry nitrogen glovebox (VAC, ≤1 ppm H_2O) at room temperature. To prepare the solutions, LiTf was dissolved into PMDETA at various concentrations and stirred for at least 4 h. A similar sample preparation was used for the PMDETA−NaTf samples, except the samples were heated to completely dissolve the salt and stirred for 24 h. The compositions of the solutions are reported as a PMDETA to salt molar ratio. At high salt compositions, the solutions contained both a liquid and a gellike phase that formed within 24 h. Eventually, all the samples became phase separated. Approximately 3 months later, a fine-grained, gritty textured material had formed at the gel−liquid interface and on the glass surface just above the sample. After about 6 months, the gel−liquid interface and on the glass surface just above the sample was composed of crystals. However, the solutions were still in a gellike phase. The crystals were allowed to completely dry in a nitrogen atmosphere. The formation of crystals was evident in most of the PMDETA−LiTf and all of the PMDETA−NaTf samples prepared. However, single crystals suitable for X-ray diffraction measurements could be isolated only from the PMDETA−NaTf samples.

2.2. X-ray Diffraction. Single crystals for X-ray analysis were grown and isolated from a $(PMDETA)_{3.3}NaTf$ solution. X-ray data were collected at 110(2) K on a Bruker Apex diffractometer, using Mo Kα radiation ($\lambda = 0.71073$ Å). The structure was solved by the direct method, using the SHELXTL system, and refined by full-matrix least squares on F^2, using all reflections. All non-hydrogen atoms were refined anisotropically, and all hydrogen atoms were included with idealized parameters. The final R1 = 0.042 is based on 7629 "observed reflections" ($I > 2\sigma(I)$), and $wR^2 = 0.107$ is based on all reflections (10798 unique reflections).

2.3. Differential Scanning Calorimetry. Single crystals of (PMDETA)NaTf weighing in total approximately 1.0 mg were sealed in a 40-μL aluminum pan. DSC data were collected with a Mettler DSC 820 calorimeter with Star^e software (v.6.10) under dry nitrogen purge. Data were collected during two heating and cooling cycles between 25 and 300 °C at a heating and cooling rate of 5 deg/min.

2.4. IR and Raman Spectroscopy. For IR measurements, the PMDETA, $(PMDETA)_x$LiTf solutions, and $(PMDETA)_x$NaTf solutions were placed between zinc selenide windows in a sealed sample holder. Finely ground powders of the PMDETA−LiTf complex and (PMDETA)NaTf crystals were prepared as KBr pellets. IR data were recorded on a Bruker IFS66V with a KBr beam splitter over a range of 500−4000 cm^{-1} (1-cm^{-1} resolution). The spectra of the solutions were measured under a dry air purge; the crystal data were collected under vacuum (8 mbar). For the Raman measurements, the PMDETA, $(PMDETA)_x$LiTf, and $(PMDETA)_x$NaTf solutions were placed in a round, aluminum sample holder and covered with a glass cover plate; single crystals of (PMDETA)NaTf were sealed in a quartz cuvette. Raman data of the solutions were recorded on a FT-Raman system (Bruker Equinox 55/FRA 106) with a CCD detector and Nd:YAG laser (1064-nm line). However, Raman data of the single crystals were recorded with a Jobin-Yvon T64000 system in the triple subtractive mode with a CCD detector, using the 532-nm line of a diode-pumped Nd:YVO_4 laser for excitation. All Raman data were collected in a 180° scattering geometry. The crystalline data were acquired with use of a laser power of 300 (crystal data) and 200 mW (solution data) measured at the laser head.

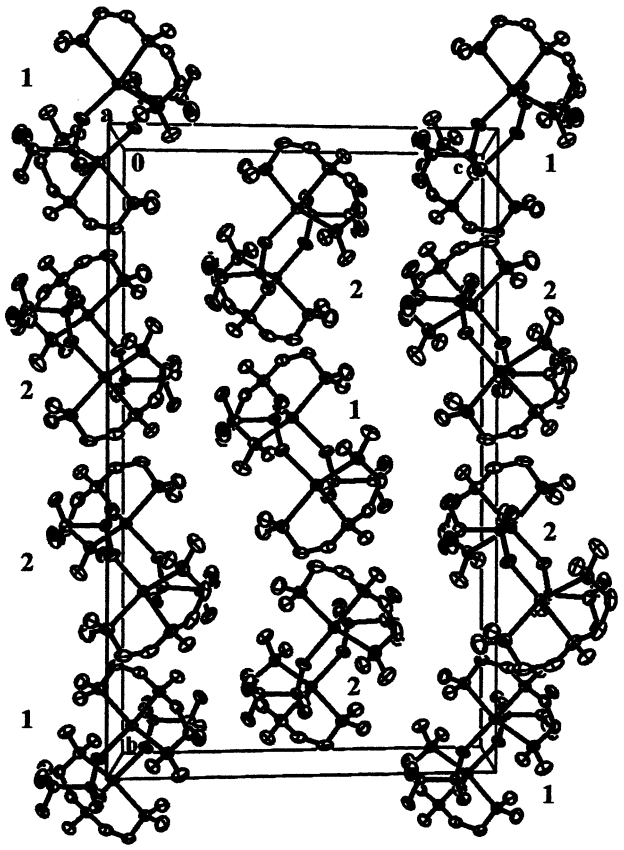

Figure 1. Packing diagram of the (PMDETA)NaTf crystal.

3. Results and Discussion

3.1. Crystal Structure. A crystal structure of the PMDETA−LiTf complex could not be determined with X-ray diffraction because a single crystal of adequate size could not be isolated. The (PMDETA)NaTf crystallizes in the monoclinic space group $P2_1/c$ with six formula units per cell (Figure 1). Therefore, the asymmetric unit of (PMDETA)NaTf consists of one and half $(PMDETA:NaTf)_2$ molecules such that there are two different kinds of dimers in the unit cell. Dimer (1) has a center of symmetry whereas dimer (2) does not. In the cell, there are two dimer (1) and four dimer (2) units, as illustrated in Figure 1. In both types of dimers, the sodium ion is coordinated to two triflate oxygen and three nitrogen atoms (Figure 2). Structural data are summarized in Table 1; selected bond lengths and angles for the crystal are listed in Tables 2 and 3. There are only a few minor differences between the bond angles and lengths of the two dimers.

The conformational structures of the PMDETA oligomers can be characterized in terms of the C−N−C−C and N−C−C−N dihedral angles (gauche, g, 60 ± 30°; gauche minus, $\bar{g}$, −60 ± 30°; trans, t, ±180 ± 30°). An individual PMDETA molecule can have a large number of different conformations because it has two N−C−C−N dihedral angles, a methyl group coordinated to the shared nitrogen atom, and two methyl groups attached to the terminal nitrogen atoms. The N−C−C−N dihedral angle is of most interest because it is directly affected by coordination of the cation to the nitrogen atoms. In the (PMDETA)NaTf crystal (Table 3), dimer (1) has only one set of N−C−C−N dihedral angles (−62.3°, 61.2°) because the PMDETA molecules are related by the inversion center. Dimer (2) has two different sets of dihedral angles for the PMDETA molecule (60.8°, −62.0°; 61.4°, −58.9°). Overall, the N−C−C−N dihedral angles in (PMDETA)NaTf are g and $\bar{g}$. The

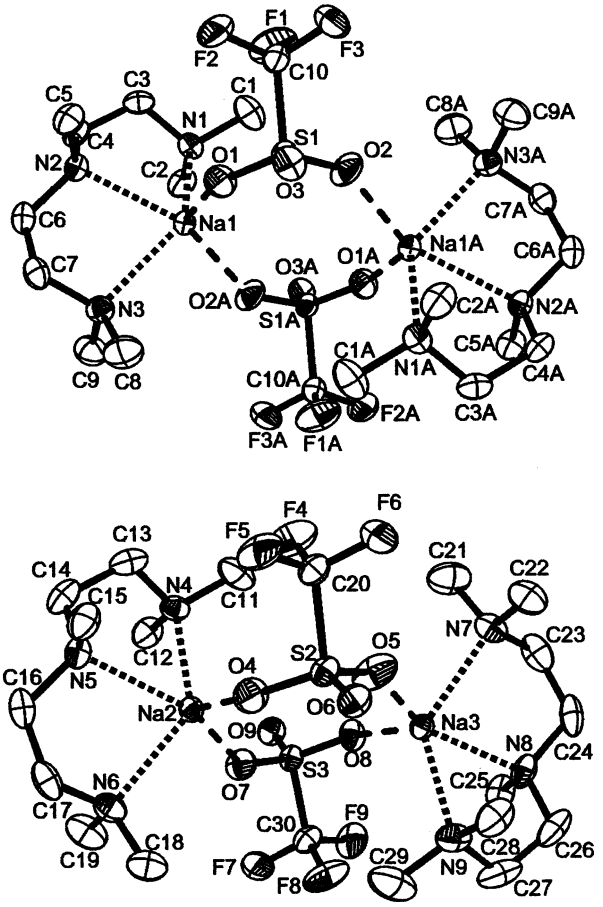

Figure 2. Dimer 1 (top) and 2 (bottom) structures in the (PMDETA)-NaTf crystal.

TABLE 1: Structural Data of the (PMDETA)NaTf Crystal

crystal system	monoclinic
space group	$P2_1/c$
temp (K)	173(2)
a (Å)	9.8001(8)
b (Å)	29.867(2)
c (Å)	17.9858(14)
α (deg)	90
β (deg)	97.4740(10)
γ (deg)	90
vol (Å^3)	5219.8 (7)
Z	6
density (Mg/m^3)	1.318
R1	0.0420
cryst size (mm^3)	0.34 × 0.18 × 0.16

conformation of both PMDETA:NaTf dimers is $x_1gx_1-x_2\bar{g}x_2$ (x_1 = t, g; x_2 = t, $\bar{g}$).

PMDETA is the nitrogen-containing analogue of diethylene glycol dimethyl ether or diglyme, $CH_3(OCH_2CH_2)_2OCH_3$. Diglyme is an oligomer of PEO and, as noted earlier, PMDETA is an oligomer of LPMEI. Each oligomer contains two repeat units of the high molecular weight polymer and can coordinate salts. Diglyme forms 1:1 compounds with NaTf[9] and with LiTf;[7] in both cases the crystal structure has been determined. Interestingly, there is a striking similarity between the structures of PMDETA−NaTf and diglyme−LiTf, rather than with diglyme−NaTf. In the 1:1 compounds PMDETA:NaTf and diglyme:LiTf, the crystals are composed of dimeric units containing two cations that are each 5-fold coordinated with three heteroatoms of the oligomer and two triflate oxygen atoms, one from each of two triflate ions. There is little resemblance between crystal structures of PMDETA−NaTf and diglyme−NaTf.

TABLE 2: Selected Bond Lengths (Å) and Angles (deg) in the (PMDETA)NaTf Crystal[a]

	dimer (1)	dimer (2)
bond length		
Na−N	2.5063 (14)	2.4758 (14)
	2.4812 (13)	2.5053 (14)
	2.4937 (15)	2.4587 (15)
		2.4792 (14)
		2.4773 (15)
		2.4937 (15)
Na−O	2.2903 (12)	2.3054 (13)
	2.2709 (13)*	2.3074 (13)
		2.2620 (13)
		2.2809 (12)
bond angle		
N−Na−N	73.88(5)	73.44(5)
	73.81(4)	74.17(5)
	133.50(5)	129.79(5)
		73.93(5)
		73.42(5)
		131.58(5)

[a] The symmetry transformation ($-x$, $-y$, $-z$ + 2) was used to generate equivalent atoms.

TABLE 3: Dihedral Angles (deg) of the (PMDETA)NaTf Crystals with Their Corresponding Conformations

bond sequence	dihedral angle	conformation
	dimer 1	
C1−N1−C3−C4	−170.15 (14)	t
C2−N1−C3−C4	69.79 (17)	g
N1−C3−C4−N2	61.06 (18)	g
C3−C4−N2−C5	77.17 (16)	g
C3−C4−N2−C6	−159.29 (13)	t
C4−N2−C6−C7	159.98 (13)	t
C5−N2−C6−C7	−76.81 (16)	$\bar{g}$
N2−C6−C7−N3	−62.32 (18)	$\bar{g}$
C6−C7−N3−C9	−73.94 (17)	$\bar{g}$
C6−C7−N3−C8	164.38 (14)	t
	dimer 2	
C11−N4−C13−C14	−172.86 (14)	t
C12−N4−C13−C14	67.28 (19)	g
N4−C13−C14−N5	60.85 (19)	g
C13−C14−N5−C15	83.39 (17)	g
C13−C14−N5−C16	−153.26 (15)	t
C14−N5−C16−C17	159.39 (14)	t
C15−N5−C16−C17	−77.40 (17)	$\bar{g}$
N5−C16−C17−N6	−62.00 (19)	$\bar{g}$
C16−C17−N6−C19	−75.59 (18)	$\bar{g}$
C16−C17−N6−C18	162.25 (14)	t
C21−N7−C23−C24	−166.61 (15)	t
C22−N7−C23−C24	72.21 (19)	g
N7−C23−C24−N8	61.49 (19)	g
C23−C24−N8−C25	75.55 (17)	g
C23−C24−N8−C26	−160.94 (14)	t
C24−N8−C26−C27	155.94 (15)	t
C25−N8−C26−C27	−80.41 (19)	$\bar{g}$
N8−C26−C27−N9	−59.1 (2)	$\bar{g}$
C26−C27−N9−C28	−67.89 (19)	$\bar{g}$
C26−C27−N9−C29	171.83 (15)	t

3.2. Thermal Analysis. Differential scanning calorimetry (DSC) was used to characterize thermal transitions in (PMDETA)NaTf. The DSC thermogram (data not shown) shows two endothermic phase transitions occurring at 104 and 237 °C in the first heating cycle. In the cooling cycle, the only thermal transition observed is at 238 °C. During the second heating cycle, there is only one transition occurring at 236 °C. In addition, this peak becomes broader and smaller, indicating a decrease in the crystallinity of the sample. However, the temperatures at which (PMDETA)NaTf melts (237 °C) and recrystallizes (238 °C) are reproducible upon cycling, within experimental error.

TABLE 4: Band Frequencies (cm^{-1}) and Assignments of PEO, LPEI, and LPMEI Complexed with LiTf and NaTf

	"free"	contact ion pair	aggregate I	aggregate II	spectrum	ref
NaTf						
PEO	753	756	761	769	Raman	30
LPEI	754	756−757	762		Raman	36
LPMEI	751−752	756	758−759		IR	21, 37
LiTf						
PEO	752−753	757	760−761		IR	7, 33−35
LPEI	752−753	755−757	759−760		Raman	36
LPMEI	752	757−758	761−762		IR	21

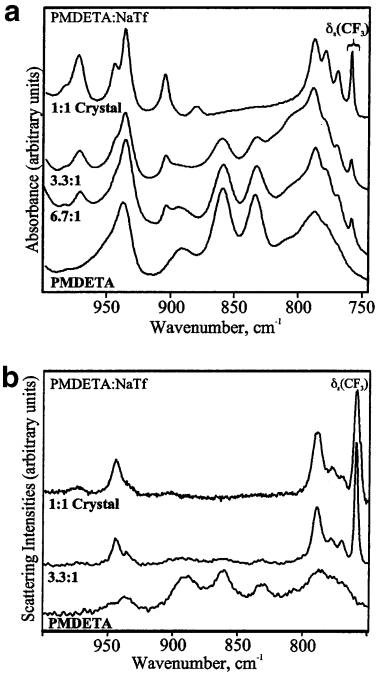

Figure 3. (a) IR spectra from 750 to1000 cm^{-1} of PMDETA, $(PMDETA)_xNaTf$ solutions ($x = 6.7$ and 3.3), and (PMDETA)NaTf. (b) Raman spectra from 750 to 1000 cm^{-1} of PMDETA, $(PMDETA)_{3.3}$: NaTf solution, and (PMDETA)NaTf crystal.

3.3. Vibrational Spectroscopy. The PMDETA−LiTf crystalline complex and (PMDETA)NaTf have distinct spectral signatures that are related to their local structures. Comparing crystalline spectral signatures to those of the amorphous phase can provide insight into the local structures present in solutions of $(PMDETA)_xLiTf$ and $(PMDETA)_xNaTf$. This work will focus on the 750 to 1200 cm^{-1} region, which contains both PMDETA and triflate modes. In the 770 to 1000 cm^{-1} region, the frequencies and intensities of the bands are particularly sensitive to conformations of the PMDETA backbone. Bands in this region have also been shown to provide information about backbone conformation in ethylene oxide-based systems.[25−30]

3.3.1. Ionic Association Region. The frequencies and intensities of the CF_3 symmetric deformation mode, $\delta_s(CF_3)$, provide information about ionically associated species. Spectral−structural correlations have been previously worked out for PEO,[7,27,30−34] LPEI,[35] and LPMEI systems complexed with LiTf and NaTf.[36] These correlations are listed in Table 4. In the salt complexes of both LPEI and LPMEI, the relative amount of aggregate species increases with increasing salt composition.

In crystalline (PMDETA)NaTf (Figure 3a,b), the $\delta_s(CF_3)$ band occurs at 759 cm^{-1} (IR and Raman). This band is due to the vibrations of triflate ions coordinated by sodium ions in a manner such that the local geometry is best described as a $[Na_2Tf]^+$ species. This frequency is slightly lower than the reported values in LPEI−NaTf and PEO−NaTf systems, but comparable to that for the LPMEI−NaTf system (see Table 4).

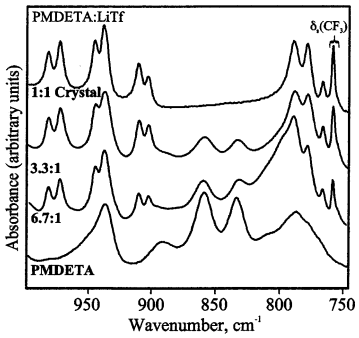

Figure 4. IR spectra from 750 to 1000 cm^{-1} of PMDETA, $(PMDETA)_xLiTf$ solutions ($x = 6.7$ and 3.3), and crystalline PMDETA−LiTf.

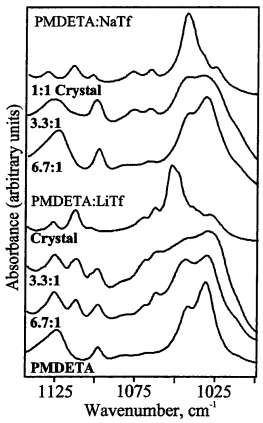

Figure 5. IR spectra from 1000 to 1200 cm^{-1} of PMDETA, $(PMDETA)_xLiTf$ and $(PMDETA)_xNaTf$ solutions ($x = 6.7$ and 3.3), crystalline PMDETA−LiTf, and (PMDETA)NaTf crystal.

In crystalline PMDETA−LiTf (Figure 4), the $\delta_s(CF_3)$ band occurs at 758 cm^{-1} (IR and Raman), which is the value observed in LPEI−LiTf systems. This band is assigned to the $[Li_2Tf]^+$ species, based on its similarity in frequency with $\delta_s(CF_3)$ in crystalline (PMDETA)NaTf. The dominant species in both the $(PMDETA)_xLiTf$ and $(PMDETA)_xNaTf$ solutions are $[M_2Tf]^+$ (M = Li, Na).

The frequency of the SO_3 symmetric stretch, $\nu_s(SO_3)$, is also affected by coordination of the triflate ion with the cation. Raman-active bands at 1032−1033, 1037−1042, and 1044−1056 cm^{-1} correspond to "free" ions, contact ion pairs, and aggregate species, respectively, in ethylene oxide-based systems complexed with LiTf.[1,7,27,32,33] Similar results are reported in poly(ethylene oxide)−NaTf systems; again there is a second aggregate species present at 1058 cm^{-1}.[30,37] In LPEI and LPMEI systems, there are no reported frequencies for the $\nu_s(SO_3)$ bands because polymer bands occur at the same frequencies as the $\nu_s(SO_3)$ bands.

In the absorbance spectra of crystalline (PMDETA)NaTf (Figure 5), the $\nu_s(SO_3)$ band occurs at ~1043 cm^{-1} (IR); in crystalline PMDETA−LiTf, this band occurs at 1048 and 1052 cm^{-1}. Studies of $\nu_s(SO_3)$ are complicated by underlying

TABLE 5: Selected IR and Raman Vibrational Frequencies (cm^{-1}) of PMDETA, (PMDETA)NaTf, and Crystalline PMDETA−LiTf

	IR						Raman			
PMDETA	770	779	787	791			769		777	786
	~807	834	859	891			831	861	890	
			937	~944			936	944		
	1031	1042	1098	~1123			1071	1098	1123	~1128
PMDETA NaTf	770	779	788	880			770		778	789
	904		936	944	972	982	~934	944		
	1065	1072					1071			
	1102	1114	1124	1130						
PMDETA LiTf	766	779	790				766	775	779	790
	903	910	938	945	973	982	937	945		
	1063	1070		1098			1075			
	1103	1112	1126							

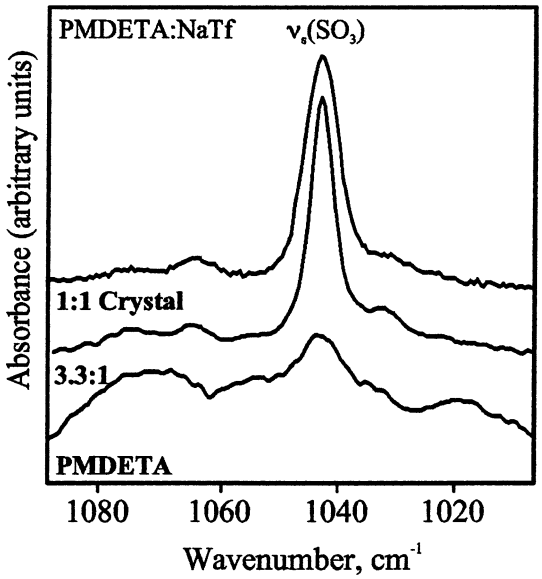

Figure 6. Raman spectra from 1000 to 1100 cm^{-1} of PMDETA, $(PMDETA)_{3.3}$NaTf solution, and (PMDETA)NaTf crystal.

PMDETA bands in the PMDETA−LiTf and PMDETA−NaTf spectra. However, the Raman spectra are relatively simple in this region. The $\nu_s(SO_3)$ mode occurs at 1049 cm^{-1} in the $(PMDETA)_x$LiTf solutions (data not shown) and 1043 cm^{-1} in PMDETA−NaTf (Figure 6). The aggregate species in (PMDETA)NaTf is dominant in the solutions, even at low triflate compositions (6.7:1; data not shown).

Utilizing standard group theoretical methods,[38] a correlation field analysis of (PMDETA)NaTf shows that the $\nu_s(SO_3)$ modes can be classified according to the irreducible representation of the $P2_1/c$ unit cell group as

$$\text{Dimer 1: } \Gamma(\nu_s(SO_3)) = A_g + B_g + A_u + B_u \quad (1)$$

$$\text{Dimer 2: } \Gamma(\nu_s(SO_3)) = 2A_g + 2B_g + 2A_u + 2B_u \quad (2)$$

In principle, there should be six Raman active components ($3A_g + 3B_g$) observed in which four components result from dimer (2). However, in the Raman spectra, only one $\nu_s(SO_3)$ band is observed (1043 cm^{-1}), indicating that the Raman-active components occur at essentially the same frequency. Therefore, there are rather small structural differences between the two dimers in (PMDETA)NaTf.

3.3.2. Conformation Region. Selected IR and Raman frequencies of PMDETA, (PMDETA)NaTf, and crystalline PMDETA−LiTf are listed in Table 5. When NaTf or LiTf is added to PMDETA, major changes occur in the spectra, such as the disappearance of PMDETA bands, the appearance of new bands, and the narrowing of bandwidths. Most striking is the disappearance of the strong bands at 834 and 859 cm^{-1} upon crystallization in both PMDETA−NaTf (Figure 3a) and PMDETA−LiTf (Figure 4), indicating a change in conformation. Similar results are evident in the Raman spectra. These solution state IR and Raman bands are due to PMDETA molecules with at least one trans N−C−C−N dihedral angle, based on quantum chemical calculations of PMDETA in the gas phase using a hybrid Hartree−Fock/density functional method (B3LYP) with a 6-31G(d) basis set.[39]

In the 750−810 cm^{-1} region, the IR and Raman bands become more intense with smaller bandwidths upon crystallization of PMDETA−LiTf and (PMDETA)NaTf. In the 900−1000 cm^{-1} region, the PMDETA band at 944 cm^{-1} (IR and Raman) does not shift in frequency upon crystallization of the two compounds. The new IR bands that form in this region become more intense with increasing salt concentration.

There are some spectroscopic differences between crystalline PMDETA−LiTf (Figure 4) and (PMDETA)NaTf (Figure 3a). The IR band at 766 cm^{-1} in PMDETA−LiTf is 4 cm^{-1} lower in frequency compared to this band in (PMDETA)NaTf (770 cm^{-1}). These bands consist of predominantly CH_2 rocking motion.[39] The two IR bands at 779 and 788 cm^{-1} in PMDETA−LiTf and 779 and 790 cm^{-1} in (PMDETA)NaTf are associated with mixed CH_2 rocking and C−N stretching motions.[39] There is a new PMDETA band at 880 cm^{-1} (IR), which only occurs in the (PMDETA)NaTf spectrum (Figure 3a). In crystalline PMDETA−LiTf, the two IR bands at 938 and 945 cm^{-1} are observed at lower frequencies in (PMDETA)NaTf (936 and 944 cm^{-1}). These bands are assigned to mixed CH_2 rocking, C−N stretching, and C−C stretching motions.[39]

3.3.3. 1000 to 1350 cm^{-1} Region. The PMDETA bands in the 1000 to 1050 cm^{-1} region are hard to isolate due to the presence of $\nu_s(SO_3)$ modes. In the Raman spectra (Figure 6), the PMDETA bands in this region are weak compared to the strong $\nu_s(SO_3)$ band. In the 1050 to 1080 cm^{-1} region, the IR bands in PMDETA−NaTf are 2 cm^{-1} lower in frequency than in PMDETA−LiTf (Figure 5; Table 5). In both PMDETA−LiTf and PMDETA−NaTf, the 1075-cm^{-1} band shifts 2 cm^{-1} higher upon crystallization. In the (PMDETA)NaTf spectra, there is a new IR band at 1114 cm^{-1}, which only forms in the crystalline phase. In both PMDETA−LiTf and PMDETA−NaTf, the intensities of the PMDETA bands (IR) at 1098 and 1124 cm^{-1} decrease upon crystallization.

The CF_3 asymmetric stretching mode occurs at 1233 cm^{-1} in crystalline PMDETA−LiTf and 1228 cm^{-1} in crystalline (PMDETA)NaTf (Figure 7). The frequencies of these bands do not change upon crystallization from solution (data not shown). The SO_3 asymmetric stretch, $\nu_{as}(SO_3)$, of the triflate ion is also affected by coordination to the cations, as illustrated in Figure

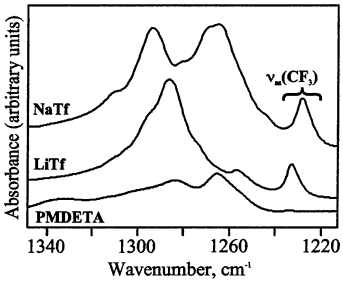

Figure 7. IR spectra from 1210 to 1350 cm^{-1} of PMDETA, crystalline PMDETA−LiTf, and (PMDETA)NaTf crystal.

7. The apparent simplicity of the PMDETA−LiTf crystal spectrum in this region is deceptive. The 2-fold degeneracy of the $\nu_{as}(SO_3)$ mode in an isolated triflate ion is broken by the potential energy environment in the crystal. Formally, each of the resulting two components in a unit cell is then correlated through intermolecular interactions, resulting in a vibrational multiplet structure that, in principle, could be analyzed by standard group theoretical methods. However, a crystal structure is not known for PMDETA−LiTf; therefore, a symmetry-based analysis cannot be performed.

The situation in the (PMDETA)NaTf crystal is more complicated. A factor group analysis shows that the irreducible representations of the $\nu_{as}(SO_3)$ modes can be classified according to the irreducible representation of the $P2_1/c$ unit cell group as

$$\text{Dimer 1: } \Gamma(\nu_{as}(SO_3)) = 2A_g + 2B_g + 2A_u + 2B_u \quad (3)$$

$$\text{Dimer 2: } \Gamma(\nu_{as}(SO_3)) = 4A_g + 4B_g + 4A_u + 4B_u \quad (4)$$

Because the sample was in the form of a microcrystalline powder, in principle all 12 infrared-active components ($6A_u + 6B_u$) could be observed in a transmission experiment. In the spectrum, prominent bands are observed at 1265, 1269, and 1293 cm^{-1}, with a smaller, asymmetric band at 1279 cm^{-1}. In addition, a very weak band occurs at 1309 cm^{-1}. The inability to observe all 12 infrared-active components may be due to small dipole moment derivatives of some factor group components, or very small correlation field splittings that leave a number of factor group components at roughly the same frequency. Without an oriented single crystal and a complete set of polarized infrared reflection spectra, a detailed assignment of these five bands in terms of their symmetry species is not possible. In the $\nu_{as}(SO_3)$ region, the spectra are also complicated by the underlying PMDETA bands.

4. Conclusions

Single crystals of (PMDETA)NaTf have been isolated and characterized with use of X-ray diffraction, DSC, IR, and Raman techniques. Local structures similar to those in the crystal are present in the (PMDETA)$_x$LiTf and (PMDETA)$_x$NaTf solutions, even at a 6.7:1 composition, demonstrating that spectroscopic studies of the PMDETA−LiTf and (PMDETA)NaTf crystals can provide insight into the local structures present in solutions of (PMDETA)$_x$LiTf and (PMDETA)$_x$NaTf. In addition, spectroscopic data show a significant change in conformation upon passing from solution to the crystalline phase. The X-ray diffraction data show that PMDETA has g-$\bar{g}$ N−C−C−N dihedral angles in the crystalline phase; quantum chemical calculations suggest that PMDETA can exist with g, t, and $\bar{g}$ N−C−C−N dihedral angles in the solution phase. The PMDETA bands in the 800 to 900 cm^{-1} region could only be assigned based on quantum chemical calculations of PMDETA with a trans N−C−C−N dihedral angle.

In (PMDETA)NaTf, the difference in the symmetries of the two kinds of dimers does not greatly affect their bond angles and lengths. As a consequence, these differences are not apparent in the IR or Raman spectra.

In (PMDETA)NaTf, the $\delta(CF_3)$ band (759 cm^{-1}) is due to the $[Na_2Tf]^+$ aggregate species. The aggregate species in crystalline PMDETA−LiTf (758 cm^{-1}) is attributed to the $[Li_2Tf]^+$ species, based on the similarity to the vibrational frequency of the $\delta(CF_3)$ band in (PMDETA)NaTf. The ionic association in (PMDETA)$_x$LiTf and (PMDETA)$_x$NaTf solutions is similar to that in the PMDETA−LiTf crystalline complex and (PMDETA)NaTf, where in solutions even at a 6.7:1 composition, the primary ionic species is $[M_2Tf]^+$ (M = Li, Na). However, this species vibrates at slightly lower frequencies (758−759 cm^{-1}) than in PEO-based electrolyte systems (761−763 cm^{-1}).

Acknowledgment. We thank Scott Boesch for the Hartree-Fock/density functional calculations of PMDETA, PMDETA−LiTf, and PMDETA−NaTf. This work was partially supported by funds from the National Science Foundation, Contract No. DMR-0072544.

References and Notes

(1) Papke, B. L.; Ratner, M. A.; Shriver, D. F. *J. Electrochem. Soc.* **1982**, *129*, 1434.
(2) Armand, M. B.; Chabagno, J. M.; Duclot, M. J. In *Fast Ion Transport in Solids*; Vashista, P., Mundy, J. N., Shenoy, G. K., Eds.; North-Holland: Amsterdam, The Netherlands, 1979; p 131.
(3) Huang, W.; Frech, R.; Johansson, P.; Lindgren, J. *Electrochim. Acta* **1995**, *40*, 2147.
(4) Bruce, P. G.; Vincent, C. A. *Faraday Discuss. Chem. Soc.* **1989**, *88*, 43.
(5) Frech, R.; Huang, W.; Dissanayake, M. A. K. L. *Mater. Res. Soc. Symp. Proc.* **1995**, *369*, 523.
(6) Kearley, G. J.; Johansson, P.; Delaplane, R. G.; Lindgren, J. *Solid State Ionics* **2002**, *147*, 237.
(7) Rhodes, C. P.; Frech, R. *Macromolecules* **2001**, *34*, 2660.
(8) Sutjianto, A.; Curtiss, L. A. *J. Phys. Chem. A* **1998**, *102*, 968.
(9) Rhodes, C. P.; Khan, M.; Frech, R. *J. Phys. Chem. B* **2002**, *106*, 10330.
(10) Rhodes, C. P. Crystalline and Amorphous Phases in Polymer Electrolytes and Model Systems. Ph.D. Dissertation, University of Oklahoma, 2001.
(11) Boesch, S.; York, S.; Wheeler, R. A.; Frech, R. *Phys. Chem. Commun.* http://hotdog.rsc.org/ej/qu/2001/B009250I/index.htm.
(12) York, S. S.; Boesch, S. E.; Wheeler, R. A.; Frech, R. *Phys. Chem. Commun.* **2002**, *5*, 99.
(13) York, S. S.; Boesch, S. E.; Wheeler, R. A.; Frech, R. *Macromolecules* **2003**, *36*, 7348.
(14) Sanders, R. A.; Frech, R.; Khan, M. A. *J. Phys. Chem. B* **2004**, *2004*, 2186.
(15) Saegusa, T.; Ikeda, H.; Fujii, H. *Macromolecules* **1972**, *5*, 108.
(16) Chatani, Y.; Irie, T. *Polymer* **1988**, *29*, 2126.
(17) Tanaka, R.; Ueoka, I.; Takaki, Y.; Kataoka, K.; Saito, S. *Macromolecules* **1983**, *16*, 849.
(18) Tanaka, R.; Fujita, T.; Nishibayashi, N.; Saito, S. *Solid State Ionics* **1993**, *60*, 119.
(19) Sanders, R. A.; Snow, A. G.; Frech, R.; Glatzhofer, D. T. *Electrochim. Acta* **2003**, *48*, 2247.
(20) Tanaka, R.; Koike, M.; Tsutsui, T.; Tanaka, T. *J. Polym. Sci.*: *Polym. Lett.* **1978**, *16*, 13.
(21) Sanders, R. A.; Snow, A. G.; Frech, R.; Glatzhofer, D. T. *Electrochim. Acta* **2003**, *48*, 2247.
(22) Sanders, R. A.; Frech, R.; Khan, M. *J. Phys. Chem B* **2003**, *107*, 8310.
(23) Sanders, R. A.; Boesch, S. E.; Snow, A. G.; Hu, L. R.; Frech, R.; Wheeler, R. A.; Glatzhofer, D. T. *Polym. Prepr.* **2003**, *44*, 996.
(24) Sanders, R. A.; Boesch, S. A.; Snow, A. G.; Hu, R. L.; Frech, R.; Wheeler, R. A.; Glatzhofer, D. T. Manuscript in progress.
(25) Frech, R.; Huang, W. *Macromolecules* **1995**, *28*, 1246.
(26) Matsuura, H.; Fukuhara, K. *J. Polym. Sci. B*: *Polym. Phys.* **1986**, *24*, 1383.
(27) Frech, R.; Huang, W. *Solid State Ionics* **1994**, *72*, 103.
(28) Goutev, N.; Ohno, K.; Matsuura, H. *J. Phys. Chem. A* **2000**, *104*, 9226.

(29) Murcko, M. A.; DiPaola, R. A. *J. Am. Chem. Soc.* **1992**, *114*, 10010.
(30) Rhodes, C. P.; Frech, R. *Solid State Ionics* **1999**, *121*, 91.
(31) Schantz, S.; Sandahl, J.; Börjesson, L.; Torell, L. M.; Stevens, J. R. *Solid State Ionics* **1988**, *28*−*30*, 1047.
(32) Huang, W.; Frech, R.; Wheeler, R. A. *J. Phys. Chem.* **1994**, *98*, 100.
(33) Frech, R.; Chintapalli, S.; Bruce, P. G.; Vincent, C. A. *Macromolecules* **1999**, *32*, 808.
(34) Seneviratne, V.; Furneaux, J.; Frech, R. *Macromolecules* **2001**, *35*, 6392.
(35) York, S.; Frech, R.; Snow, A.; Glatzhofer, D. *Electrochim. Acta* **2001**, *46*, 1533.
(36) Sanders, R. A.; Frech, R. *J. Phys. Chem. B* **2002**, *107*, 8310.
(37) Kakihana, M.; Schantz, S.; Torell, L. M. *Solid State Ionics* **1990**, *40/41*, 641.
(38) Fateley, W. G.; Dollish, F. R.; McDevitt, N. T.; Bentley, F. F. *Infared and Raman Selection Rules for Molecular and Lattice Vibrations*: *The Correlation Method*; John Wiley & Sons: New York, 1972.
(39) Boesch, S.; Wheeler, R. A., Vibrational Mode Assignments of PMDETA, PMDETA−LiTf and PMDETA−NaTf. Private communication.